Atomic and electronic structure of thin films of Mn on Pd{111}

D. Tian, H. Li,* S. C. Wu,† and F. Jona
College of Engineering and Applied Science, State University of New York, Stony Brook, New York 11794

P. M. Marcus
IBM Thomas J. Watson Research Center, P.O. Box 218, Yorktown Heights, New York 10598
(Received 25 September 1991)

Epitaxial films of Mn can be grown on Pd{111} to thicknesses of the order of 15–20 layers. Vacuum deposition on a room-temperature substrate produces a threefold-symmetric 1×1 phase with in-plane lattice constant $a=2.75$ Å (pseudomorphic to Pd{111}) and bulk interlayer spacing $d_{\text{bulk}}=2.16$ Å. This structure probably corresponds to strained magnetic γ-Mn. Vacuum deposition on a 150°C substrate produces a sixfold-symmetric $\sqrt{3}\times\sqrt{3}$-30° structure, which is probably a bulk phase with in-plane lattice constant $a=4.76$ Å. The atomic structure of this phase is unknown, but may be related to α-Mn.

I. INTRODUCTION

In work reported earlier[1,2] we have shown that thin films of a metastable body-centered-tetragonal phase of Mn can be grown epitaxially at room temperature on Pd{001} substrates to thicknesses of the order of 20 layers. The lattice parameters of this phase as grown are $a=2.75$ Å (which is the edge of the primitive unit mesh on Pd{111}, the cubic lattice constant of fcc Pd is $a_0=3.89$ Å) and $c=3.43$ Å. This phase results from a 2.5–3 % distortion of a tetragonal phase determined with x rays in Mn-rich γ-MnCu alloys[3] ($a_0=3.78$ Å, $c/a_0=0.938$), γ-MnPt alloys[3] ($a_0=3.79$ Å, $c/a_0=0.96$), or γ-MnFe (Ref. 4) ($a_0=3.796$ Å, $c/a_0=0.945$). The tetragonality is expected in type-I antiferromagnets [the spin direction is reversed in alternate (001) planes, which breaks the cubic symmetry].[5]

The present report concerns a study of the growth of Mn on a Pd{111} substrate, the experimental tools being low-energy electron diffraction (LEED), Auger-electron spectroscopy (AES), and ultraviolet photoemission spectroscopy. In general, investigations of the growth of a given adsorbate on different crystallographic surfaces of the same substrate material are interesting because they permit studies of the effect of variations of the adsorbate-substrate interactions with respect to adsorbate-adsorbate interactions: different surfaces can produce different results. For example, Cu films grow epitaxially to thicknesses of the order of 10 layers on both Pd{001} and Pd{111}, but they do so pseudomorphically with about 8% strain on Pd{001} (Ref. 6) and incommensurately with no strain on Pd{111}.[7]

The case of Mn on Pd is particularly interesting because the tetragonal phase found for Mn on Pd{001} is not expected to fit on a {111} surface of a fcc crystal. We will see, in fact, that Mn films can grow pseudomorphically on Pd{111} with a trigonally distorted fcc structure, and that a new phase with a $\sqrt{3}$-times-larger lattice constant in the surface plane can be grown at temperatures somewhat higher than room temperature.

We present in Sec. II the experimental procedures, in Sec. III the experimental observations, in Sec. IV the structure analyses done on the grown Mn films, in Sec. V the photoemission studies, and in Sec. VI the discussion of the results.

II. EXPERIMENT

The Pd sample was a $10\times5\times1$-mm^3 platelet with one of the two major surfaces oriented perpendicular to a ⟨111⟩ direction and polished to a mirror finish. The sample was mounted on a manipulator that allowed variations of both the polar (θ) and the azimuthal (ϕ) angle of incidence of the electron beam in a LEED apparatus. The Pd{111} surface was cleaned *in situ* (base pressure $\leq7\times10^{-11}$ Torr) with cycles of Ar-ion bombardments (200–800 eV, 20 μA, 5×10^{-5} Torr, about 1 h) followed by anneals at 800°C (20 min). After 10 cycles the sample surface was clean: AES showed, in particular, no detectable C, O, or S signals above the noise level. The LEED pattern of the clean surface was a sharp threefold symmetric 1×1 pattern with low background.

The Pd{111} sample could be rotated to face a Mn source consisting of a tungsten spiral that was partially covered with premelted Mn and could be heated by passage of an electric current. Deposition of Mn on the Pd{111} surface was typically done with the source at about 1200° C at a pressure of 1.5×10^{-10} Torr or better. The Mn coverage was determined from the ratio $R=I_{\text{Mn(589)}}/I_{\text{Pd(330)}}$ between the intensities of the Mn and Pd AES lines at 589 and 330 eV, respectively, with the formula

$$R=R_\infty\frac{1-e^{-d/\lambda_{589}}}{e^{-d/\lambda_{330}}}, \tag{1}$$

where $R_\infty=I^\infty_{\text{Mn(589)}}/I^\infty_{\text{Pd(330)}}=0.23/0.8=0.29$ (Ref. 8); I^∞ denotes the intensity of the AES line from a very thick sample of Mn (Pd) at 589 (330) eV; the λ's are the

inelastic mean free paths of electrons with 589 (330) eV energy traveling in Mn [$\lambda_{589}=13.1$ Å, $\lambda_{330}=9.8$ Å (Ref. 9)], and d is the thicknesses of a film Mn assumed to be uniform over the Pd{111} surface. The AES scans were done with a cylindrical mirror analyzer (CMA). The thicknesses of the Mn films as determined with Eq. (1) are quoted, below, in layer equivalents (LE), representing the number of *uniformly distributed* layers of Mn that would produce the same value of the ratio R in Eq. (1) as that measured in the actual experiments. The conversion from d in Å to d in LE was done by assuming an interlayer distance of 2.16 Å, as determined below. The error bars in the determination of film thickness are estimated to be about ±50%.

III. EXPERIMENTAL OBSERVATIONS

In most experiments, the rate of deposition of Mn was determined to be 1 Å/min, or about 1 LE in 2–2.5 min. At this rate, and with the substrate at room temperature, the LEED pattern remained 1×1 and threefold symmetric with increasing surface coverage, but both the background and the size of the diffracted beams increased monotonically until a coverage of about 5–6 LE was reached, and remained about the same thereafter. Similarly, the LEED $I(V)$ curves (measured with a TV camera and computer combination[10]) changed continuously with increasing surface coverage up to 5 or 6 LE and remained stable thereafter. The thickest 1×1 Mn film grown in these experiments was about 16 LE thick. The LEED intensity analysis described below was done with a film about 8–9 LE thick.

It is important to mention that in order to determine the changes of the LEED pattern with coverage, the deposition of Mn was done in installments of about 1 min each (about 0.5 LE) separated by time intervals of about 30–40 min between successive depositions. During these time intervals, devoted to various LEED and AES measurements, the Mn source was not heated. Different results were obtained if the deposition of Mn was done *continuously* over a time period of about 30 min, producing films with thicknesses between 13 and 14 LE. In this case the LEED pattern was $\sqrt{3}\times\sqrt{3}$-30° with *sixfold symmetry*. The maximum intensities of the "fractional-order" beams were about the same as those of the "integral-order" beams, suggesting that the pattern was probably *not* due to reconstruction of the surface, but rather produced by a bulk film with an in-plane lattice constant $\sqrt{3}$ times larger than that of Pd{111}; i.e., an in-plane lattice constant $a=\sqrt{3}\times 2.75=4.76$ Å. These observations were reproducible: Mn films with thicknesses larger than about 8 or 9 LE gave a threefold symmetric 1×1 LEED pattern if they were produced by short successive depositions spaced about 0.5 h apart (with the Mn source turned off between depositions), but gave a sixfold symmetric $\sqrt{3}\times\sqrt{3}$-30° LEED pattern if they were produced by a single deposition lasting about 30 min.

Seeking an explanation for this behavior, we considered three possibilities, viz., (1) more impurities could have been produced by the out-gassing of the source and its surroundings during the long uninterrupted depositions than during the several short depositions—these impurities may have been responsible for the occurrence of different structures; (2) although during each deposition (i.e., whenever the Mn source was hot and the substrate was exposed to it) the rate was the same, the *effective* deposition rate was different in the two cases considered—different arrival rates of the Mn atoms may have caused the change in structure; and (3) in the course of the long uninterrupted deposition the substrate may have been heated by radiation from the hot source (about 10 cm away), whereas during the short, widely spaced depositions the substrate was always at room temperature—the structural change may have been triggered by different temperatures.

Possibility (1) was negated by a study of the AES spectra collected in both series of experiments. After the growth of 10- to 15-LE films, the levels of contamination typically reached 2 at. % (mostly oxygen) no matter how the depositions were made. Thus, impurities were not responsible for the occurrence of different structures. Possibility (2) was negated by a new series of experiments in which the temperature of the Mn source was decreased to about 900 °C, thereby reducing the deposition rate by about a factor of 4, but the deposition was still made in a long uninterrupted installment. At the end the LEED pattern was still $\sqrt{3}\times\sqrt{3}$-30°, suggesting therefore that the difference in effective deposition rates, as least within a factor of 4, was not responsible for the occurrence of two different structures. Possibility (3) appeared to be most probable on the basis of a new series of experiments. The substrate was heated to 150 °C and deposition was made in installments of 1–5 min each, separated by 30-min periods. The $\sqrt{3}\times\sqrt{3}$-3− 30° structure was formed, and, in fact, the slow growth allowed a study of the evolution of the structure.

Thus, with the substrate at 150 °C it was established that the $\sqrt{3}\times\sqrt{3}$-30° beams became visible at about 3 LE, although the LEED pattern had still threefold symmetry (arising from the Pd{111} substrate that was still visible to the probing electrons). By the time the surface coverage reached 7–8 LE, the symmetry of the LEED pattern was wholly sixfold. AES scans showed that the Pd signal decreased steadily with increasing coverage, but was still present in 7- to 8-LE Mn films [recall that the relative AES sensitivity of Pd is 3–4 times larger than that of Mn (Ref. 8)]. The LEED pattern was at its best, i.e., the intensity of the LEED beams and the signal-to-background ratio in the $\sqrt{3}\times\sqrt{3}$-30° structure were largest, for Mn films with thicknesses between 8 and 15 LE. In the thicker films the Pd AES signal was no longer detectable. However, with increasing thickness the background increased steadily and the beams broadened: 20-LE films exhibited very high background and broad LEED spots.

We conclude that the $\sqrt{3}\times\sqrt{3}$-30° structure of the Mn films (more precisely, a structure epitaxial to Pd{111}, but with in-plane lattice constant equal to 4.76 Å and sixfold symmetry) was preferentially formed when the temperature of the substrate was a little higher than room temperature, say, between 50 and 150 °C.

IV. STRUCTURE ANALYSES

LEED $I(V)$ spectra were collected for normal and non-normal incidence of the primary beam from 8- to 9-LE Mn films with the 1×1 structure and from 10- to 12-LE Mn films with the $\sqrt{3}\times\sqrt{3}$-30° structure. The LEED intensity calculations were carried out with the CHANGE computer program;[11] the Mn potential was taken from the compilation of Moruzzi, Janak, and Williams;[12] eight phase shifts and 55 beams were used for calculations of the 1×1 structure up to 360 eV; the inner potential was chosen as $V_0=-(10+4i)$ eV, and the root-mean-square amplitude of the atomic vibrations was set at $\langle u^2\rangle^{1/2}=0.125$ Å. Evaluation of the correspondence between experiment and theory was done both visually and with the reliability factors $R_{\rm VHT}$ (Ref. 13), $R_{\rm P}$ (Ref. 14), and $r_{\rm ZJ}$.[15]

A. Mn{111} 1×1

We discuss first the analysis of the 1×1 structure. The calculations were done for a semi-infinite Mn{111} crystal with the in-plane lattice constant a of Pd{111} ($a=2.75$ Å) and with variable bulk and surface interlayer spacings. The bulk interlayer spacing $d_{\rm bulk}$ was varied in the initial stages between 1.7 and 2.5 Å (for Pd{111}, $d_{\rm bulk}=2.246$ Å) in steps of 0.1 Å, and in later stages between 1.74 and 1.86 Å, and between 2.04 and 2.19 Å in steps of 0.03 Å. For all values of $d_{\rm bulk}$ the first interlayer spacing, d_{12}, was relaxed from a contraction of 0.2 to an expansion of 0.2 Å in steps of 0.05 Å.

Minimization of the R factors gave widely differing results, namely $R_{\rm VHT}$ was minimized to 0.46 for $d_{\rm bulk}=1.96$ Å and Δd_{12} (the change in d_{12}) equal to $+0.2$ Å; $R_{\rm P}$ was minimized to 0.47 for $d_{\rm bulk}=2.18$ Å and $\Delta d_{12}=0$; and $r_{\rm ZJ}$ was minimized to 0.17 for $d_{\rm bulk}=2.27$ Å and $\Delta d_{12}=-0.17$ Å. The contour plots of the three R factors in the Δd_{12}-$d_{\rm bulk}$ plane, depicted in Fig. 1, show, however, that the minima are shallow. All three R factors have maxima in the region around $d_{\rm bulk}=2.0$ Å and $\Delta d_{12}=0$, and all three have low values along a valley extending from ($d_{\rm bulk}=2.1$ Å, $\Delta d_{12}=+0.15$ Å) to ($d_{\rm bulk}=2.3$ Å, $\Delta d_{12}=-0.2$ Å), where the values of the R factors vary from 0.54 to 0.48 for $R_{\rm VHT}$, from 0.60 to 0.50 for $R_{\rm P}$, and from 0.24 to 0.18 for $r_{\rm ZJ}$. Thus, all three reliability factors exhibit similar behavior, although the absolute minima vary considerably from one another. We ascribe this inconsistency among R factors to the defects and disorder that produce the large background and broad spots observed in the LEED pattern and smear the intensity peaks in the $I(V)$ spectra. The visual evaluation of the agreement between calculations and experiment picks the $I(V)$ curves calculated with $d_{\rm bulk}=2.16$ Å and $\Delta d_{12}=0$ (hereafter referred to as model 1) as the ones providing the best fit to experiment. Theoretical and experimental curves are juxtaposed in Fig. 2.

The smearing effect of disorder can also be seen in the effect of limited long-range order in the films is difficult to investigate quantitatively. We have nevertheless attempted to simulate a situation in which both the in-plane lattice constant and the interlayer spacing fluctuate around mean values by calculating $I(V)$ curves from films with

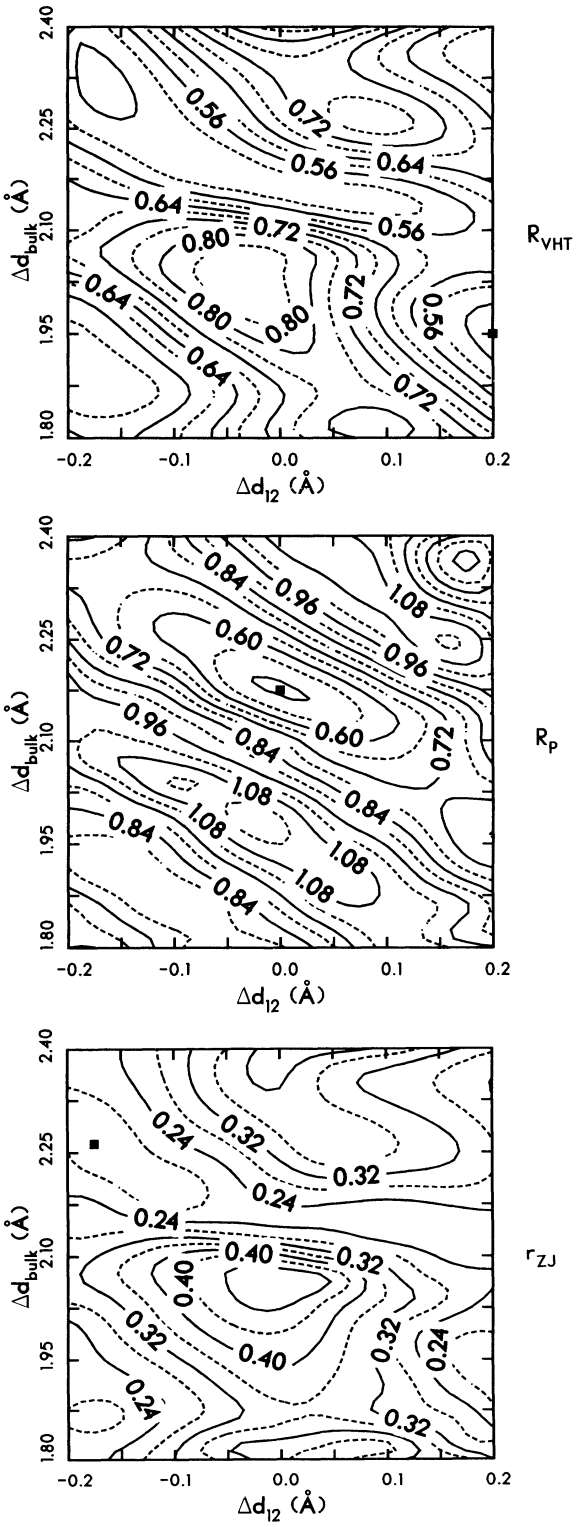

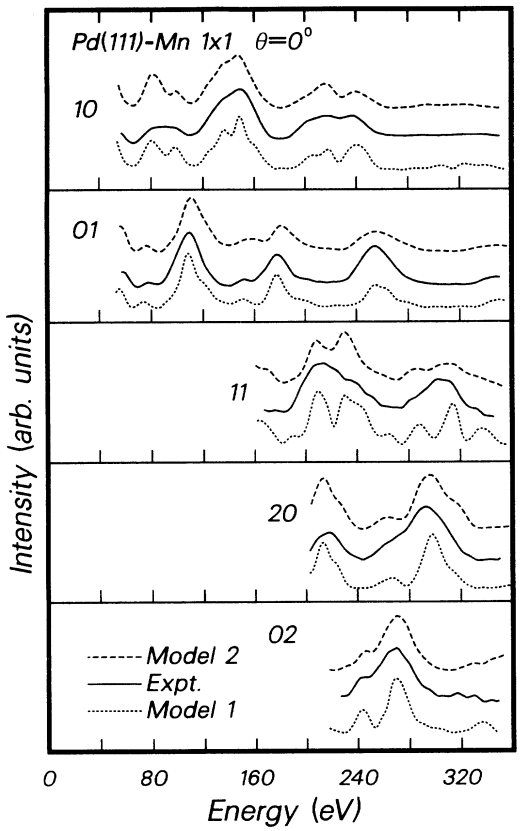

FIG. 2. Experimental (solid) and theoretical LEED $I(V)$ spectra for the LEED intensity analysis of a 9-LE film of 1×1 Mn on Pd{111}. Modes 1 and 2 are described in the text.

in-plane lattice constants of 2.75, 2.72, and 2.69 Å and d_{bulk} values of 2.16, 2.19, and 2.22 Å, and adding them. The resulting curves are compared to experiment in Fig. 2 (curves marked model 2) and are obviously a better fit to experiment than those of model 1, as confirmed by much lower values of the R factors: $R_{\text{VHT}}=0.23$, $R_{\text{P}}=0.28$, and $R_{\text{ZJ}}=0.07$. We thus quote the results of this structure analysis of the 1×1 films with larger-than-usual error bars as in-plane lattice constant $a=2.75\pm0.06$ Å, $d_{\text{bulk}}=2.16\pm0.06$ Å, and $\Delta d_{12}=0\pm0.06$ Å.

B. Mn {111} $\sqrt{3}\times\sqrt{3}$-30°

Two major questions must be answered before a structure analysis of the $\sqrt{3}\times\sqrt{3}$-30° structures can be attempted, namely (1) is the $\sqrt{3}\times\sqrt{3}$-30° structure a *surface* superstructure over an otherwise 1×1 bulk, or simply a *bulk* structure with in-plane lattice constant $\sqrt{3}$ times larger than that of Pd{111}, and (2) what is the cause of the sixfold symmetry of the $\sqrt{3}\times\sqrt{3}$-30° LEED pattern?

Final answers are now known at this time, but some suggestions can be made. Qualitative observations of the relative intensities of "fractional-order" and "integral-order" beams seem to indicate, as mentioned above, that the $\sqrt{3}\times\sqrt{3}$-30° structure is one of a *bulk* film with in-plane lattice constant $a=4.76$ Å (Pd does not seem to participate in the $\sqrt{3}\times\sqrt{3}$-30° structure, as its signal is not present in AES scans of $\sqrt{3}\times\sqrt{3}$-30° Mn films thicker than about 9 or 10 LE). However, it is difficult to relate this value of a to simple Mn structures, i.e., to either fcc (γ-) or bcc (δ-) Mn. On the basis of mere misfit to the Pd{111} substrate (see discussion below), a strained bcc structure of the grown films may perhaps be considered. Thus, for purposes of comparison to experiment, we calculated the LEED $I(V)$ curves expected from semi-infinite bcc Mn{111} with in-plane lattice constant $a=4.76$ Å and bulk interlayer spacings varying between 2.2 and 0.4 Å in steps of 0.1 Å. (The number of beams had to be increased to 163 at 300 eV in order to do these calculations.)

However, a {111} surface of δ-Mn would have threefold, not sixfold symmetry, which brings us to the second question asked above. In general, if the structure of the film were cubic (either fcc or bcc, in either case with ABCABC... stacking), sixfold symmetry could be explained only by the presence of 180° domains in equal concentrations. If the structure of the film were hexagonal, with ABAB... stacking, then sixfold symmetry would be explained more naturally by the presence of monoatomic steps on the surface.[16] However, domain averaging of our calculations on δ-Mn did not produce agreement with experiment, and calculations on hexagonal Mn were not attempted.

V. PHOTOEMISSION STUDIES

The main purpose of the photoemission studies was to examine whether the obvious difference in atomic structure between the 1×1 and the $\sqrt{3}\times\sqrt{3}$-30° phases was reflected in a difference in electronic structure as well.

The photoemission experiments were carried out on beamline U7B at the National Synchrotron Light Source at Brookhaven National Laboratory. The synchrotron radiation was dispersed by means of a plane-grating monochromator and the photoelectron energies were measured by means of a CMA either in the angle-resolved mode with an angular resolution of 2° or in the angle-integrated mode. A three-axis manipulator[9] allowed variations of the polar, azimuthal, and tilt axes of the sample under study in such a way that photoemission experiments could be done with s- or ($75\%s+25\%p$)-polarized radiation.

We collected valence-band photoemission spectra from both the 1×1 and the $\sqrt{3}\times\sqrt{3}$-30° Mn/Pd{111} films in both the angle-resolved and angle-integrated modes. We show in Fig. 3 (top) two representative electron-distribution curves (EDC's) measured with s-polarized 90-eV photons at normal emission. The EDC from the 1×1 structure features a pronounced peak at about -4 eV, whereas the EDC from the $\sqrt{3}\times\sqrt{3}$-30° structure exhibits instead a broad peak around -3 eV. Angle-integrated EDC's (not shown) are found to be similar to their angle-resolved counterparts.

Thus, the difference in atomic structure detected by LEED is extended here to a difference in electronic structure. A little more can be said, in fact, about the $\sqrt{3}\times\sqrt{3}$-30° phase. Sugawara *et al.*[17] have published

angle-integrated EDC's from high-purity films of α-Mn (the stable room-temperature modification) for photon energies between 30 and 130 eV. We find our EDC's measured on the $\sqrt{3}\times\sqrt{3}$-30° structure to be similar to the curves published by Sugawara *et al.*,[17] suggesting therefore that the $\sqrt{3}\times\sqrt{3}$-30° phase is similar to α-Mn. Thus these results indicate that the density of states in the valence band of the $\sqrt{3}\times\sqrt{3}$-30° phase is similar to that of α-Mn and quite different from that of the 1×1 phase.

However, the magnetic moments of the Mn atoms are essentially the same in the two structures. Figure 3 (bottom) shows that the splittings of the 3*s* levels in the 1×1 and $\sqrt{3}\times\sqrt{3}$-30° structures are the same within experimental error. The magnitude of the splitting is 5.6 eV, which is larger than the value 4.08 eV measured on polycrystalline α-Mn films by McFeely *et al.*[18] with x-ray photoemission spectroscopy. Using the same analysis as these authors, we find that the "spin-only" magnetic moment is about $3.9\mu_B$ (i.e., 56% larger than the value $2.5\mu_B$ found by McFeely *et al.*[18] in α-Mn). Such an enhanced moment may be due to the volume expansion associated with the epitaxial strain. We note that the magnitude of the 3*s* splitting (5.6 eV) is about the same as that found in MnF_3.[19]

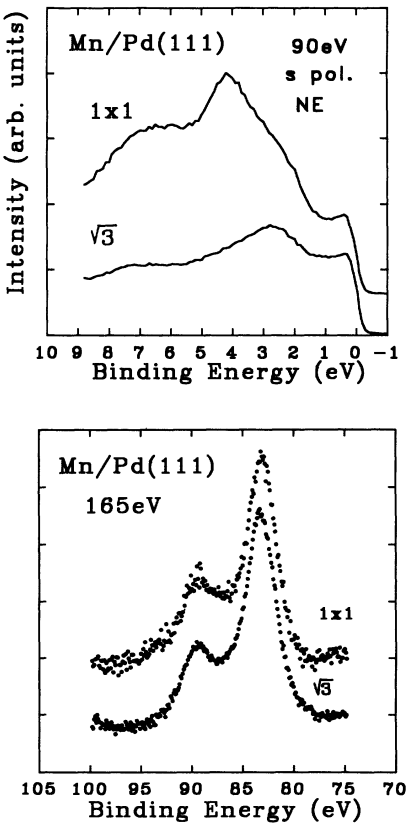

FIG. 3. Top: Angle-resolved normal-emission electron-distribution curves measured with *s*-polarized 90-eV photons on a 20-LE film of Pd{111}-(1×1)-Mn and on a 12-LE film of Pd{111} $\sqrt{3}\times\sqrt{3}$-30° Mn. Bottom: 3*s* core levels for both films mentioned above.

VI. DISCUSSION

The Mn films deposited on room-temperature Pd{111} are both pseudomorphic and epitaxial. The actual structure of the films is not strictly fcc, because the in-plane lattice constant is determined by the substrate (2.75 Å), but the bulk interlayer spacing (2.16 Å) is 3.8% smaller than that of Pd{111} (2.25 Å). Since the elastic constants of fcc Mn are not known, a strain analysis of the structure is not possible, and therefore the equilibrium (i.e., the unstrained) phase cannot be determined with certainty. But it is quite probable that the equilibrium phase is γ-Mn. The lattice constant of (fcc) γ-Mn at room temperature is $a_0=3.73$ Å when extrapolated from temperatures above 1095 °C (Ref. 1) and therefore has a misfit of 4.2% to Pd's a_0 of 3.89 Å.

We recall that, on Pd{001}, Mn films grow pseudomorphically and epitaxially as a tetragonal phase with pseudocell parameters $a_0=3.81$ Å and $c/a_0=0.938$ (Refs. 1 and 2), and that Mn crystals stabilized by small amounts of impurities have a tetragonal structure with pseudocell parameters $a_0=3.79$ Å and $c/a_0=0.938$ (Refs. 3 and 4), the tetragonal distortion being related to the antiferromagnetism that lowers the energy below the minima of the ferromagnetic (FM) and nonmagnetic (NM) phases. However, on a cubic {111} surface such as Pd{111}, the growth of a tetragonal phase does not seem possible (there would be no threefold symmetry), whereas the growth of strained metastable (fcc) γ-Mn is consistent with the observed threefold symmetry.

The magnetic state of the grown films may be inferred from comparisons with theory. Spin-polarized total-energy calculations[20] find $a_0=3.51$ Å for NM γ-Mn at room temperature, involving a volume per atom of 10.8 Å.[3] The experimental value of the atomic volume (calculated from the unit-mesh rhombus on {111} with $a=2.75$ Å and $d_{\text{bulk}}=2.16$ Å) is 14.15 Å^3, hence markedly larger than that calculated for NM γ-Mn. The expansion from the NM value is very probably due to a magnetic moment of the Mn atoms. We can therefore infer that the grown Mn films were magnetic, either ferromagnetic (for which theory[20] finds $a_0=3.87$ Å) or, more probably, antiferromagnetic. The magnetic state appears to be different from the film grown on Pd{001}, with a volume per atom of 12.98 Å^3.

The nature and the origin of the Pd{111} $\sqrt{3}\times\sqrt{3}$-30° Mn structure, which can be grown on 150°C substrates, are more obscure. From the point of view of lattice misfit alone, the δ phase of Mn appears to be the closest to the $\sqrt{3}\times\sqrt{3}$-30° phase. Extrapolation of the δ-Mn lattice constant $a_0=3.08$ Å at 1134 °C to room temperature gives a room-temperature value of $a_0=2.98$ Å (Ref. 1), but spin-polarized total-energy calculations[20] find $a_0=2.79$ Å for NM δ-Mn and $a_0=3.11$ Å for FM δ-Mn. In the latter case, the lattice constant in a {111} plane would be 4.40 Å, or about 8% smaller than the observed 4.76-Å value.

Thus the lattice constant of metastable FM δ-Mn is the closest of the simple Mn structures to that of the $\sqrt{3}\times\sqrt{3}$-30° phase. Nevertheless, the growth of films as thick as 20 LE with 8% strain is very improbable, and

there still remains the problem that the grown $\sqrt{3}\times\sqrt{3}$-30° films have sixfold, not threefold, symmetry, therefore requiring the existence of domains. At room temperature the stable structure of Mn (α-Mn) is the cubic $A12$ structure[3] with $a_0=8.91$ Å and 58 atoms per unit cell. This structure is very complicated, although the atomic arrangement is not a great departure from a bcc structure[21] and may perhaps be distorted in such a way as to fit on a 4.76-Å hexagonal mesh, but it would still be only threefold symmetric and therefore require the presence of rotationally different domains. It is of interest, in this respect, to note that the photoemission data indicate that the $\sqrt{3}\times\sqrt{3}$-30° phase is electronically similar to the α phase. A structure analysis with surface x-ray diffraction may possibly shed some light on the atomic structure of the $\sqrt{3}\times\sqrt{3}$-30° phase.

Finally, we note that there is probably a connection between the results reported here and those reported by Heinrich and co-workers (Refs. 22 and 23) for Mn on Ru(0001). On Ru(0001), Mn was reported to grow epitaxially and pseudomorphically to a thickness of 2–3 layers and *then* to form a 3×1 or a $\sqrt{3}\times\sqrt{3}$-30° phase, which Heinrich *et al.* tentatively identified as having either the hexagonal Zn_2Mg or the fcc Cu_2Mg structure, both similar to the more complex α-Mn structure. The difference between the Mn/Pd{111} and the Mn/Ru(0001) systems is that in the former case we could grow either the 1×1 or the $\sqrt{3}\times\sqrt{3}$-30° phase, depending on the substrate temperature, whereas in the Mn/Ru(0001) case the two phases were observed to grow sequentially at the same temperature of about 60 °C. Perhaps this difference may be due to the fact that, on Pd{111} ($a=2.75$ Å), Mn is strained more than on Ru(0001) ($a=2.70$ Å). The larger strain may also explain why, on Pd{111}, the splitting of the Mn $3s$ levels (5.6 eV) is larger than on Ru(0001) (the precise value is not quoted in Refs. 22–24, but the figures suggest a splitting of about 4.6 eV).

ACKNOWLEDGMENTS

We are grateful to the U.S. National Science Foundation and to the U.S. Department of Energy for partial support of this work under Grant Nos. DMR-89-21123 and DE-FG02-86ER45239, respectively. One of us (S.C.W.) is also indebted to the National Natural Science Foundation of the People's Republic of China for partial support through Grant No. 19074004.

*Present address: The BOC Group, Technical Center, Murray Hill, NJ 07974.

†On leave from Department of Physics, Peking University, The People's Republic of China.

[1]D. Tian, S. C. Wu, F. Jona, and P. M. Marcus, Solid State Commun. **70**, 199 (1989).

[2]F. Jona and P. M. Marcus, Surf. Sci. **223**, L897 (1989).

[3]W. B. Pearson, *A Handbook of Lattice Spacings and Structures of Metals and Alloys* (Pergamon, Oxford, 1967).

[4]Y. Endoh and Y. Ishikawa, J. Phys. Soc. Jpn. **30**, 1614 (1971).

[5]T. Oguchi and A. J. Freeman, J. Magn. Magn. Mater. **46**, L1 (1984).

[6]H. Li, S. C. Wu, D. Tian, J. Quinn, Y. S. Li, F. Jona, and P. M. Marcus, Phys. Rev. B **40**, 5841 (1989); *The Structure of Surfaces III* (Springer, New York, 1991), p. 328.

[7]H. Li, D. Tian, F. Jona, and P. M. Marcus, Solid State Commun. **77**, 651 (1991).

[8]L. E. Davis, N. C. MacDonald, P. W. Palmberg, G. E. Riach, and R. E. Weber, *Handbook of Auger Electron Spectroscopy* (Physical Electronic Industries, Inc., Eden Prairie, MN, 1978).

[9]M. P. Seah and W. A. Dench, Surf. Interface Anal. **1**, 2 (1979).

[10]F. Jona, J. A. Strozier, Jr., and P. M. Marcus, in *The Structure of Surfaces,* edited by M. A. Van Hove and S. Y. Tong (Springer, Berlin, 1985), p. 92.

[11]D. W. Jepsen, Phys. Rev. B **22**, 5701 (1980); **22**, 814 (1980).

[12]V. L. Moruzzi, J. F. Janak, and A. R. Williams, *Calculations of Electronic Properties of Metals* (Pergamon, New York, 1978).

[13]M. A. Van Hove, S. Y. Tong, and M. H. Elconin, Surf. Sci. **64**, 85 (1977).

[14]J. B. Pendry, J. Phys. C **13**, 937 (1980).

[15]E. Zanazzi and F. Jona, Surf. Sci. **62**, 61 (1977).

[16]H. D. Shih, F. Jona, D. W. Jepsen, and P. M. Marcus, J. Phys. C **9**, 1405 (1976).

[17]H. Sugawara, A. Kakizaki, I. Nagakura, and T. Ishii, J. Phys. F **12**, 2929 (1982).

[18]F. R. McFeely, S. P. Kowalczyk, L. Ley, and D. A. Shirley, Solid State Commun. **15**, 1051 (1974).

[19]J. C. Carver, G. K. Schweitzer, and T. A. Carlson, J. Chem. Phys. **57**, 973 (1972).

[20]V. L. Moruzzi, P. M. Marcus, and J. Kübler, Phys. Rev. B **39**, 6957 (1989).

[21]R. W. G. Wyckoff, *Crystal Structures* (Interscience, New York, 1963), Vol. 1.

[22]B. Heinrich, C. Liu, and A. S. Arrott, J. Vac. Sci. Technol. B **3**, 766 (1985).

[23]B. Heinrich, A. S. Arrott, C. Liu, and S. T. Purcell, J. Vac. Sci. Technol. A **5**, 1935 (1987).

[24]A. S. Arrott, B. Heinrich, C. Liu, and S. T. Purcell, J. Magn. Magn. Mater. **54-57**, 1025 (1986).